Catena 176 (2019) 159–169

Contents lists available at ScienceDirect

Catena

journal homepage: www.elsevier.com/locate/catena

Response of lower Yellow River bank breachings to La Niña events since 924 CE

Jiongxin Xu[a,*], Fuxing Li[b]

[a] Institute of Geographic Sciences and Natural Resources Research, Key Laboratory for Water Cycle and Land Surface Processes, Chinese Academy of Sciences, Beijing 100101, China

[b] College of Resources and Environmental Sciences, Hebei Normal University, Shijiazhuang 050024, China

ARTICLE INFO

Keywords:
Historical river changes
River course shifting
Hydrological effect of ENSO
Yellow River

ABSTRACT

The El Niño/Southern Oscillation (ENSO) is the dominant mode of inter-annual climate variability, strongly affecting summer precipitation and streamflow of large rivers. So far, no effort has been made to relate ENSO events with alluvial river stability. Based on the historical document of the lower Yellow River (LYR) and the data of previously reconstructed ENSO variability, the present study aims to establish the relation between the LYR's artificial levee breaching events (LBEs) and the ENSO events from 924 CE to 1938, and thereby reveal how river instability responds to climate change in millennial scale, for a better understanding of the coupling relation between the climate, hydrology and river channel changes. From 924 CE to 1938, there are 303 La Niña influenced years (ENSO variability < -0.5), of which 172 (56.8%) are related to the occurrence of LBE. We divided the reconstructed ENSO variability into 9 classes and calculated the LBE frequency for each class. We found that the LBE frequency is negatively correlated with class average value of ENSO variability, significant at $p < 0.05$. By relating the 21 major course shifting events (CSEs) of the LYR (924 CE to 1938) to the occurrence of La Niña influenced years, we found that 13 (61.9%) were influenced by La Niña. The decadal LBE frequency (F_b) and decadal average of ENSO amplitude show anti-phase variations since 1100 CE, with $r = -0.356$ ($n = 82$, $p = 0.0010$) after a linear detrending treatment. Through the control on summer rainfall and therefore on floods in the Yellow River, La Niña events influence the occurrence of the LBEs and CSEs in the LYR.

1. Introduction

The El Niño/Southern Oscillation (ENSO) is the dominant mode of interannual climate variability on Earth, alternating between anomalously warm (El Niño) and cold (La Niña) conditions in the tropical Pacific at intervals of 2–8 years (D'Arrigo et al., 2005; Deser et al., 2010). The amplitude of ENSO variability affects the occurrence and predictability of climate extremes around the world (McPhaden et al., 2006; Tang et al., 2008). Although the ENSO circulations occur on the equatorial Pacific Ocean, they may cause climatic anomalies over three quarters of the Earth surface (Jones, 1988; Kiladis and Diaz, 1989; Long and Li, 1999). In particular, the eastern equatorial Pacific sea surface temperature (SST) variability seriously affects the weather and climate over vast area of China (Dong and Liu, 2000; Li et al., 2000; Zhu et al., 2000) and the ENSO events have significant impact on occurrence of floods and their magnitude and frequency (Chang and King, 1999; Dilley and Heyman, 1999; Ward et al., 2014; Liu et al., 2017). In the upper Yellow River, El Niño events are usually associated with dry years and La Niña with wet years (Lan et al., 2002). In the past 50 years, the extreme rainfall events decreased over the Yellow River basin, which can be related with the ENSO variations (Fu et al., 2013). As the strongest interannual signals in climate systems, the occurrence and development of ENSO may cause global atmospheric circulation anomalies, leading to global climate change and natural disasters. Jiang et al. (2006) carried on a comprehensive study of major flood disasters in the world during the period 1950–2004, finding a close relation between flood disasters and global ENSO years. The relation between ENSO and flood disasters has been well established (Chang and King, 1999; Dilley and Heyman, 1999; Lan et al., 2002. Chiew and McMahon (2002) studied the ENSO-streamflow teleconnection globally, based on data from 581 catchments worldwide, suggesting that the ENSO-streamflow relationship can be used to successfully forecast streamflow.

A few papers have been published on the river channel shifting in timescales of millennium or longer. Jotheri et al. (2016) studied the Holocene avulsions of the Euphrates River in the Najaf Area of Western Mesopotamia and identified five main avulsion cycles in the past

* Corresponding author.
E-mail address: xujx@igsnrr.ac.cn (J. Xu).

https://doi.org/10.1016/j.catena.2019.01.012
Received 14 March 2018; Received in revised form 4 November 2018; Accepted 9 January 2019
Available online 21 January 2019
0341-8162/ © 2019 Elsevier B.V. All rights reserved.

5000 years. They discussed the impacts of these avulsions on human settlement pattern, but did not relate them with possible climate changes. Working from the headwaters of the White Nile to the lower White Nile valley and the valley of the desert Nile, Woodward et al. (2015) reconstructed the changes in geomorphology and flood regime over the past fifteen to twenty thousand years, including the shifting river channels. Wang and Su (2013) studied the influence of solar activity on breaching, overflowing and course-shifting events of the lower Yellow River (LYR) in the late Holocene, and found that 75.5% of the LYR course-shifting events and 61.7% of the breaching and overflowing events occurred in sunspot number decline phases of 11-year solar cycles, which caused heavy rainfall in the middle reaches of Yellow River. Chen et al. (2015) developed a new numerical model to explore the manner in which climate change and human activity have affected the flood dynamics of the Yellow River during the last 3000 years. However, no effort so far has been made to relate long term channel changes with ENSO events. Through the effect on streamflow and flood disasters, the ENSO may further affects river stability because the alluvial river channel changes usually occur during floods. The Yellow River has been regarded as "the cradle of Chinese civilization". The earliest record of the river's instability expressed by bank-breaching and course-shifting events can be traced back to 602 BCE (WGYRCC, 1982; Xu, 2001; Wang and Su, 2013), from which the information of river instability can be extracted. Based on the North American Drought Atlas, a database of drought reconstructions based on tree-ring records, Li et al. (2011) produced a continuous, annually resolved record of ENSO variability from 910 CE to 2002, which is in broad agreement with independent, ENSO-sensitive proxy records in the Pacific and surrounding regions. The present study will aims to: (1) establish the relation between the lower Yellow River's bank breachings and the ENSO events since 924 CE and (b) reveal how river instability responds to climate change and other factors, for a better understanding of the coupling relation between the climatic, hydrological and river channel systems.

2. Study area

The Yellow River (Fig. 1), 5464 km in length and ~730,000 km^2 in drainage area, crosses China's three largest landform steps known as the Qinghai-Tibet Plateau, Loess Plateau and North China Plain and then pours into the Pacific Ocean. The climate of the river basin is controlled by Asian Monsoon circulation system (Xu, 2012). From northwest to southeast, the river crosses cold alpine, arid, semi-arid and sub-humid zones. The basin-averaged mean annual precipitation is 467 mm and the natural water yield is 58 billion m^3/yr (Zhao, 1996). With the highest specific sediment yield of the world, the river transported 1.6 billion t of sediment annually to its lower reaches (from Mengjin to the sea) during the period 1919–1959, of which 0.4 billion t deposited in the channel, making the lower Yellow River (LYR) channel rise at a rate of 6 cm–10 cm annually (Chien and Zhou, 1965). Therefore, the upper reach of the LYR has a highly instable, braided channel, shifting rapidly and frequently within the two artificial levees. The construction of artificial levees started 2300 years ago during the Warring Period (475–221 BCE) (Editorial Commission for Physical Geography in China, 1982; Xu, 2001) and afterward, the sedimentation is limited between the two levees and therefore a "hanging" or "suspended" channel formed, several meters higher than the ground surface behind the levee. After the "hanging channel" developed, the LYR becomes even more instable, and artificial levee breachings occurred frequently. According to the Yellow River Water Conservancy Commission (1959), during the 3000 years before 1946, the bank and artificial levee breachings occurred 1593 times, and major course shifts occurred 26 times.

3. Data and methodology

3.1. Data sources

3.1.1. The LBE and CSE data

The channel instability may be classified as two types: levee breaching event (LBE) and river course shifting event (CSE). The LBE may be further divided as two sub-types, LBE_1 and LBE_2. The LBE_1 was caused by an over-levee flood that breached the levee. The occurrence of a LBE_2 needs three conditions: a flood whose highest water level nearly reached but was lower than the levee top, the main streamflow perpendicularly attacked the artificial levee, and the levee's strength is very weak. The flood discharge related with a LBE_2 is smaller than that with LBE_1. When the levee was breached during a large flood, large area of the alluvial plain was inundated and a serious disaster occurred, causing great loss of life and property. Following such a LBE, if the breaching failed to be closed by people, the river would shift to a new

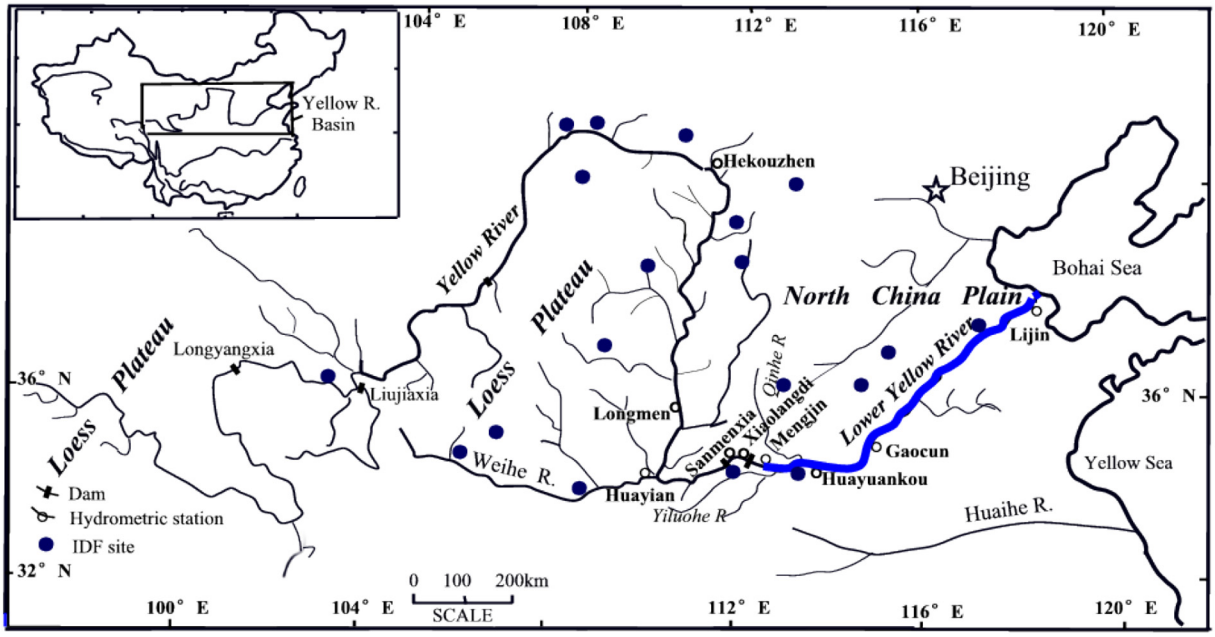

Fig. 1. The Yellow River basin. The lower Yellow River is highlighted by thick line.

course, and thus, a CSE occurs.

In the past 2000 years, the occurrence of LBE_1 and LBE_2 were documented with annual resolution, providing valuable data for studying the LYR's channel instability and course change. Because the material used to build the artificial levee is alluvium consisting of silt, fine sand and a little clay, the levee's anti-erosion ability is poor. The LBE_1 is caused by large floods beyond human control. When it occurs, the responsibility of local government officials is relatively small and the punishment to them is not serious. The LBE_2 is more related with the quality of artificial levee, and when it occurred, the officials would face serious punishment, even death penalty. Hence, they often gave false information to the central government by reporting a LBE_2 as a LBE_1. Therefore, the reported number of LBE_2 is less than what actually occurred, while the number of LBE_1 is more. For this reason, we did not make differentiation between LBE_1 and LBE_2 during the statistical analysis. A chronology has been made by the Writing Group of "A Brief History of Yellow River Water Conservancy" (WGYRCC, 1982), in which each LBE_1 and LBE_2 is listed and described in detail. In the ancient China up to 1911, a lunar calendar was used, and since 1911 when the Public of China was founded, the Gregorian calendar is the official calendar. In the above mentioned chronology of levee breachings, all the years in the historical records of LBEs were transposed to the years in Gregorian calendar. The course shift event in 602 BCE is the earliest record bank breaching in history, and the levee breaching in 1938 was the last one when the Chinese troop broke the artificial levee at Huayuankou in order to stop the Japanese intrusion. Based on these data, we determined the years in which a LBE occurred and the years in which no LBE occurred, referred to as LBE years and non-LBE years thereafter. The details of the LBE information recorded by the historical document are different. For many years, there was only one site at which the levee breaching was recorded. Hence, we did not consider how many LBEs occurred within a year and how many breaching sites along the LYR that were caused by a given LBE. A chronology of LBE years from 924 CE to 1938 is shown in Table S-1 of Appendix A (cited from WGYRCC (1982)), which are used in the present study. Based on the chronology, we also counted the number of LBE years for each decade, and then calculated the LBE frequency (F_b, in year/decade), which is used as an indicator of historical river channel instability. The F_b data are over the period from the 920 CE to 1930s. In the time series, each decade is represented by the mid-year of the decade. The LYR course shifting events (CSEs) in history were studied by the Yellow River Water Conservancy Commission (1959), who identified 26 CSEs since 602 BCE.

3.1.2. The ENSO data

There are a number of published data of ENSO reconstruction, e.g., the data by Braganza et al. (2009) for the period 1525 CE–1982, the data by Cook et al. (2009) for the period 1300 CE–1979 and the data by Li et al. (2011) for the past 1000 years. Of these data, the time series of ENSO variability reconstructed by Li et al. (2011) is the longest, and significantly ($p < 0.001$) correlated with the time series of ENSO variability reconstructed by Braganza et al. (2009) and with the time series of Nino 3.4 reconstructed by Cook et al. (2009) (see Fig. 2A and B). Hence, we used the ENSO data of Li et al. (2011) in the present study.

The ENSO variability affects the occurrence and predictability of climate extremes around the world (Li et al., 2011). Using the North American Drought Atlas (Cook et al., 2004, 2008)—a database of drought reconstructions based on tree-ring records, Li et al. (2011) produced a continuous, annually resolved record of ENSO variability (referred to as $ENSO_{Li}$ in the present study). The record by Li et al. (2011) is in broad agreement with independent, ENSO-sensitive proxy records in the Pacific and surrounding regions. The data (Li et al., 2011) are downloaded from IGBP PAGES/World Data Center for Paleoclimatology (Data Contribution Series # 2011-064: ftp://ftp.ncdc.noaa.gov/pub/data/paleo/treering/reconstructions/enso-li2011.txt), including

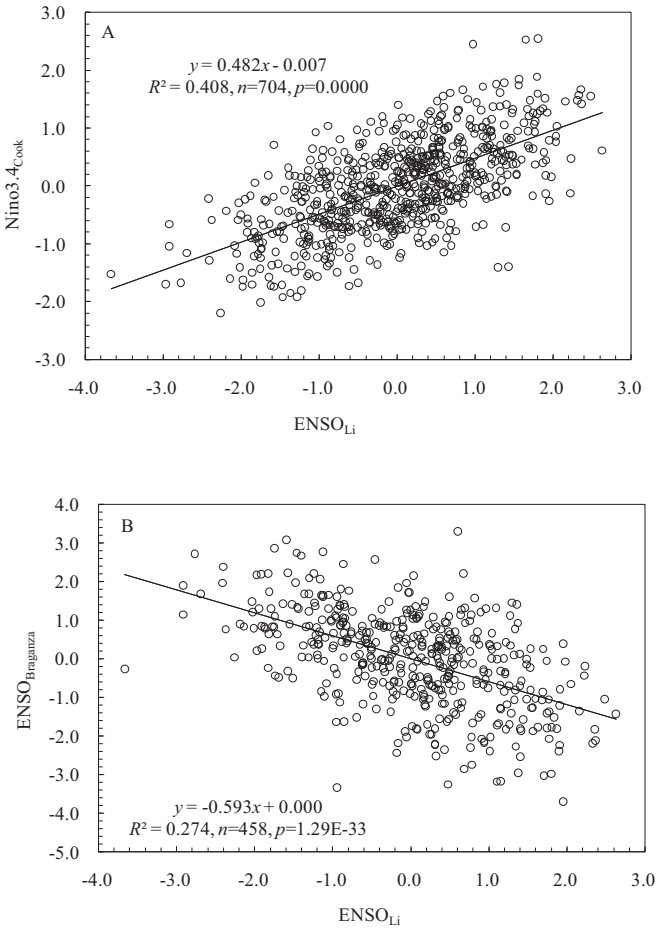

Fig. 2. Plots of $ENSO_{Li}$ against $Nino3.4_{Cook}$ (A) and $ENSO_{Braganza}$ (B). $ENSO_{Li}$ and $ENSO_{Braganza}$ are referred to as the ENSO reconstructed by Li et al. (2011) based on tree ring records, and Braganza et al. (2009) based on tree ring and ice-core records, respectively. $Nino3.4_{Cook}$ is the Nino3.4 reconstructed by Cook et al. (2009) based on tree ring records.

the interannual ENSO variability data (900 CE–2002) and the ENSO amplitude data (910 CE–1992). The overlap period of these data with the LYR LBE data is from 924 CE to 1938, which were used in the present study.

3.1.3. The IDF data

The data of Drought and Flood Index (IDF) (1470–2000) are used in the present study, which is defined as a measure of precipitation in the main precipitation season as a result of historical document analysis. This index uses five grades: 1—very wet, 2—wet, 3—normal, 4—dry, and 5—very dry, to describe moisture conditions (Zhang, 1988). The grades for the period 1470–1950 were compiled based on a statistical evaluation of historical descriptions (CMA, 1981). The values for the period 1951–2000 were converted from observed summer precipitation, assuming that this distribution of the relative frequencies of five grades is consistent through the historical times and observed times (CMA, 1981; Zhang, 1988; Yi et al., 2012). The IDF data from 120 sites in China are available from CMA (1981) and Zhang (1988), of which 19 sites are located in or neighboring the Yellow River basin, including Hohhot, Shangba, Etok, Datong, Taiyuan, Linfen, Changzhi, Anyang, Luoyang, Zhengzhou, Lanzhou, pingliang, Tianshui, Yinchuan, Yulin, Yanan, Xian, Dezhou and Jinan. These IDF data are used in the present study. The IDF from 1470 CE to 1938 are used because the LBEs data ended in 1938.

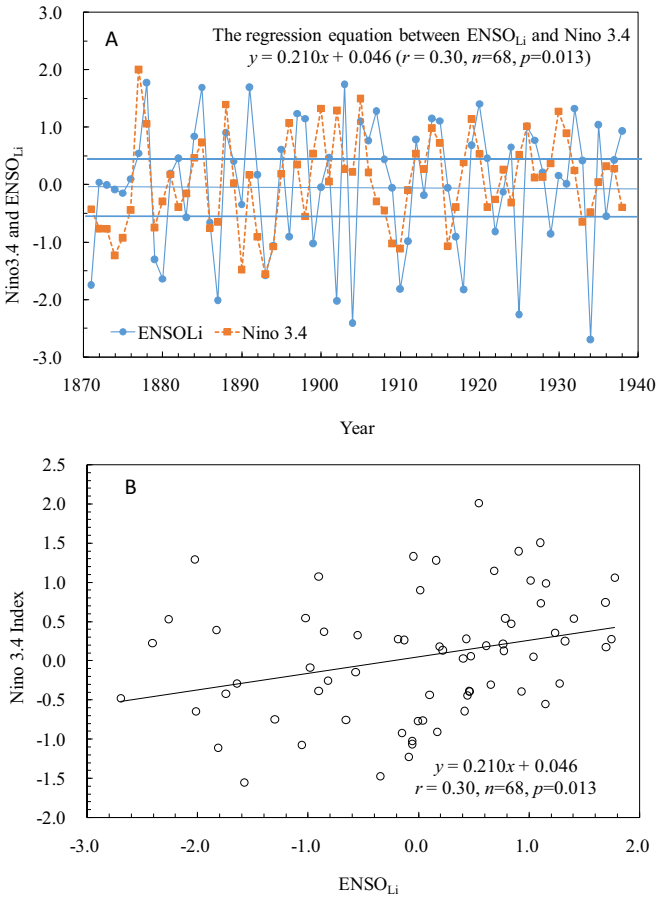

Fig. 3. (A) The variations in the annual $ENSO_{Li}$ and normalized annual Niño 3.4 Index. The Niño 3.4 data are downloaded from the Climate Diagnostics Center, National Center for Atmospheric Research, U.S., at: http://www.cgd.ucar.edu/cas/catalog/climind/TNI_N34. The two thick lines indicate ± 0.5. (B) Plot of Niño 3.4 against $ENSO_{Li}$.

3.2. Methodology

ENSO variability reflects the amplitude of the related tropical ocean SST. When the positive SST anomaly reaches a critical value, an El Niño event is thought to occur; when the negative SST anomaly reaches a critical value, a La Niña event is thought to occur (D'Arrigo et al., 2005; Deser et al., 2010). Niño 3.4 Index has been widely used to quantify the ENSO event. Based on monthly data of Niño 3.4, an El Niño and event was defined when the threshold of 0.4 °C is exceeded and a La Niña event is defined when the threshold of −0.4 °C is exceeded (Trenberth, 1997). Because only annual data of $ENSO_{Li}$ are available, we define the La Niña influenced year based on annual $ENSO_{Li}$. The temporal variations in the $ENSO_{Li}$ and Niño 3.4 Index are shown in Fig. 3A. Because the Niño 3.4 Index is available since 1870, and the LBE data are ended in 1938, we choose the period 1870–1938 to make a comparison between the $ENSO_{Li}$ and Niño 3.4 Index. It is seen that the annual $ENSO_{Li}$ and annual Niño 3.4 Index (calculated as the average of monthly Niño 3.4 Index over 12 months) show in-phase variations, the correlation coefficient between the two series is significant at $p = 0.013$ and their ranges are comparable. Therefore, we take the $ENSO_{Li} < -0.5$ as the criteria for a year influenced by La Niña; for simplicity, we call such a year as "La Niña influenced year" hereafter. Taking the overlap period (924 CE–1938) of the $ENSO_{Li}$ and LBE time series for study, we determine the La Niña influenced year one after another, which forms a time series of La Niña influenced years. Then, we make a comparison between the time series of the LBE years with the time series of the La Niña influenced years. Many researchers noted that there is a lag effect after an El Niño year or a La Niña influenced year, namely, an El Niño or a La Niña event may cause drought or flood in the same year and/or in the following year (Zou and Ni, 1997; Chiew et al., 1998; Hao et al., 2007; Lin and Lu, 2009; Li et al., 2015). As a La Niña influenced year may very likely make the Yellow River's precipitation or streamflow higher than average in the same and/or in the following year (Lan et al., 2002; Hao et al., 2007), a LBE would likely occur in the same and/or in the following year. Therefore, given a La Niña influenced year, the following four possibilities would occur: (1). The LBE occurs both in the La Niña influenced year and the following year; (2). The LBE occurs only in the La Niña influenced year; (3) The LBE occurs only in the following year; (4). No LBE occurs in the La Niña influenced year and the following year. Therefore, we may quantify the above four situations by coding them as 3, 2, 1 and 0, respectively, meaning that the response of LBE to La Niña event is at the third- (strong), second- (moderate), first (weak) and zero (non) levels, respectively. When the situations of 3, 2 and 1 occur, we may think that a La Niña event gives rise to a LBE; when the situation of 0 occurs, we may think that a La Niña event has no influence on LBE. The codes 3, 2, 1 and 0 may be called the LBE-ENSO responding index (LERI).

According to the above definitions, 303 La Niña influenced years were identified for the period from 924 CE to 1938. Then we determined the LBE-ENSO responding index for each year. We classified the La Niña influenced years into several classes in terms of $ENSO_{Li}$ and the count the number (N_{LBE}) of the related LBE years in each class, and then calculate the average value of $ENSO_{Li}$ for each class. On this basis, we calculated the frequency of LBE years (F_b, in %) of each class: $F_b = (N_{LBE} \times 100) / N_C$, where N_C is the number of years of each $ENSO_{Li}$ class. Then, the correlation between F_b and averaged $ENSO_{Li}$ of each class is established, to reveal the influence of ENSO variability on F_b. To match the F_b, we also calculated the $ENSO_{Li}$ and ENSO amplitude for each decade and then make comparison between the temporal variations in F_b and the $ENSO_{Li}$ and ENSO amplitude, by which to reveal the influence of La Niña on F_b.

The method of tele-connection analysis is used to reveal the mechanism of how the La Niña events control the occurrence of LBEs based on the observed data from 1951 to 2006. Because of highly strengthened artificial levees since 1950, the LBEs never occurred afterward. Therefore, we used the precipitation and water discharge to reflect the possible hazard of LBEs, assuming that the present artificial conditions are similar to those in history. Because the water diversion by people greatly reduced the measured water discharge, the naturalization treatment is performed to get the natural water discharge by adding back the diverted water amount. The tele-connection analysis involves in a number of atmospheric circulation variables such as the Nino 3.4 index (Trenberth and Stepaniak, 2001), an index for ENSO, the SST anomaly of the West Pacific Pool (WPWPTA) index (Zhang et al., 2009), the indices of Asian Summer Monsoon indices including the Eastern Asian Summer Monsoon index (Guo et al., 2004) and the Indian Summer index (Wang and Fan, 1999), and the water cycle variables such as precipitation over the Yellow River basin and natural water discharge in the LYR. Through this tele-connection analysis, a cause-effect chain will be proposed.

To detect the periodicities in the time series of $ENSO_{Li}$ and F_b, we performed period analysis using the method of continuous wavelet transform (CWT) analysis. If there are some common periods in the $ENSO_{Li}$ and F_b time series, it may be thought that the $ENSO_{Li}$ variability may be the cause of the F_b variability. The CWT employs wavelet functions to expand the time series into the time-frequency space to find its localized intermittent periodicities (Torrence and Webster, 1999). The wavelet functions are a class of functions with zero means localized in both frequency and time. Different types of wavelet functions can be applied in the CWT analysis. Among them, the Morlet wavelet function can provide reasonable localization in both the time and frequency space, and is therefore adopted in the present study. For more details of Morlet wavelet analysis, please see Grinsted et al. (2004).

Table 1
The LBE frequency for the 9 $ENSO_{Li}$ classes.

	Class	$ENSO_{Li}$ range	Number of years in each class	LBE years in each class	The LBE frequency for each class (%)
For the La Niña influenced years	Class 1	< −2.00	24	17	70.8
	Class 2	−2.000 to −1.75	30	18	60.0
	Class 3	−1.75 to −1.50	23	21	91.3
	Class 4	−1.50 to −1.25	26	21	80.8
	Class 5	−1.25 to −1.00	56	39	69.6
	Class 6	−1.00 to −0.75	74	35	47.3
	Class 7	−0.75 to −0.50	70	46	65.7
For the years with $ENSO_{Li}$ between −0.5 and 0	Class 8	−0.50 to −0.25	70	35	50.0
	Class 9	−0.25–0	101	40	39.6

4. Results

4.1. The response of LBE to La Niña events

Following the method described earlier, we determined the LERI for 303 La Niña influenced years with $ENSO_{Li} < -0.5$ from 924 CE to1938 (see Table S-2 of Appendix A). Of the 303 years, 57, 62, 53 and 131 have the LERI of 3, 2, 1 and 0, respectively. This means that there are 57 years in which the LBE occurred both in the La Niña influenced year and the following year; there are 62 years in which the LBE occurred only in the La Niña influenced year; there are 53 years in which the LBE occurred only in the following year of the La Niña influenced year; there are 131 years in which no LBE occurred either in the La Niña influenced year or in the following year of it. The first three types of years total 172. Hence, of the 303 La Niña influenced years, 172 (56.8%) are related to the occurrence of LBE.

To reveal the relation between the La Niña intensity and the LBE frequency (F_b), we classified the 303 La Niña influenced years into 7 classes, counted the number of LBE years and calculated the F_b for each class (see Table 1), and calculated the class average value of $ENSO_{Li}$. To make comparison in a wider range of $ENSO_{Li}$, we also considered the 171 years with $ENSO_{Li}$ between −0.5 and 0 and divided them into two classes, classes 8 and 9, and then calculated the F_b and the class averaged value of $ENSO_{Li}$ for them. Based on data from the 9 classes, the F_b is plotted against the class average value of $ENSO_{Li}$ (Fig. 4). The regression equation is: $y = 45.04e^{-0.26x}$ ($R^2 = 0.500$, $n = 9$, $p = 0.046$), significant at $p < 0.05$, which indicates that the increased intensity of La Niña (i.e., the smaller $ENSO_{Li}$), may cause a higher LBE frequency.

4.2. The LYR course shifting events (CSEs) in response to La Niña

The Yellow River Water Conservancy Commission (1959) identified 26 CSEs since from 602 BCE to 1938, of which 21 occurred from 924 CE to 1938. The 21 CSEs are listed in Table 2, where the $ENSO_{Li}$ in the same year and previous year are also shown. Some research results

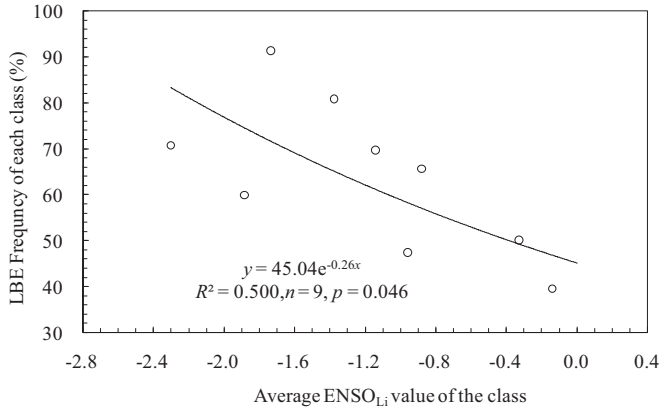

Fig. 4. The plot of LBE frequency against the class averaged $ENSO_{Li}$.

Table 2
The influence of La Niña on 21 CSEs. Note that No. 7 and No. 21 are man-induced CSEs.

No	The year of CSE	$ENSO_{Li}$ in the same year	$ENSO_{Li}$ in the previous year	Whether the CSE is influenced by La Niña (yes or no)
1	955	0.2	−1.9	Yes
2	1020	0.6	−0.7	Yes
3	1034	0.6	0.4	No
4	1048	−1.2	0.5	Yes
5	1060	1.0	−0.9	Yes
6	1081	−1.2	0.3	Yes
7	1128	1.5	−0.2	No
8	1194	−0.7	−0.4	Yes
9	1168	−0.5	0.9	Yes
10	1286	−0.2	−0.2	No
11	1297	−0.8	−0.9	Yes
12	1344	0.0	0.1	No
13	1391	0.3	−1.0	Yes
14	1416	−0.6	−1.0	Yes
15	1448	−0.3	0.4	Yes
16	1489	−0.1	−1.1	Yes
17	1509	0.7	0.3	No
18	1534	0.0	−0.2	No
19	1558	−0.4	0.5	No
20	1855	−1.2	0.5	Yes
21	1938	0.9	0.4	No

show that the occurrence of an El Niño or La Niña event will significantly affect the drought and flooding situations and summer precipitation in the same and/or following year in Asian Monsoon areas of China (Zou and Ni, 1997; Chiew et al., 1998; Hao et al., 2007; Lin and Lu, 2009; Li et al., 2015), and the similar lagging effect on CSEs can be expected. The table shows that, of the 21 CSEs, 13 occurred under the influence by La Niña, namely, the $ENSO_{Li} \leqq -0.5$ occurred either in the same year or one year before the CSE, accounting for 61.9% of the total CSEs. It should be pointed out that the No.7 CSE in 1938 and No.21 CSE in 1128 CE were caused by the army for military purpose during a war. In 1128 CE, the army of the Song Dynasty dug up the artificial levee in order to prevent the southward intrusion of the army of the Jin Dynasty. Following the levee breaching, a course shift occurred, and the Yellow River took over the channel of Huaihe River and flowed into the Yellow Sea. In 1938 during the Second World War, the Chinese army dug up the Yellow River artificial levee at Huayuankou under the order of Chiang Kai-Shek, the president of the Republic of China, to prevent the Japanese army from intrusion to the south of the Yellow River. Then, the Yellow River changed its course to the Huaihe Rive again and flowed into the Yellow Sea. As shown in Table 2, the two CSEs were not the La Niña influenced years. If these two man-induced CSE is excluded, the total CSEs should be 19 and then the CSEs under the influence of La Niña account 68.4% of the total CSEs.

4.3. Influence of ENSO amplitude on the LBE frequency of LYR

As mentioned earlier, many studies show that the ENSO is an

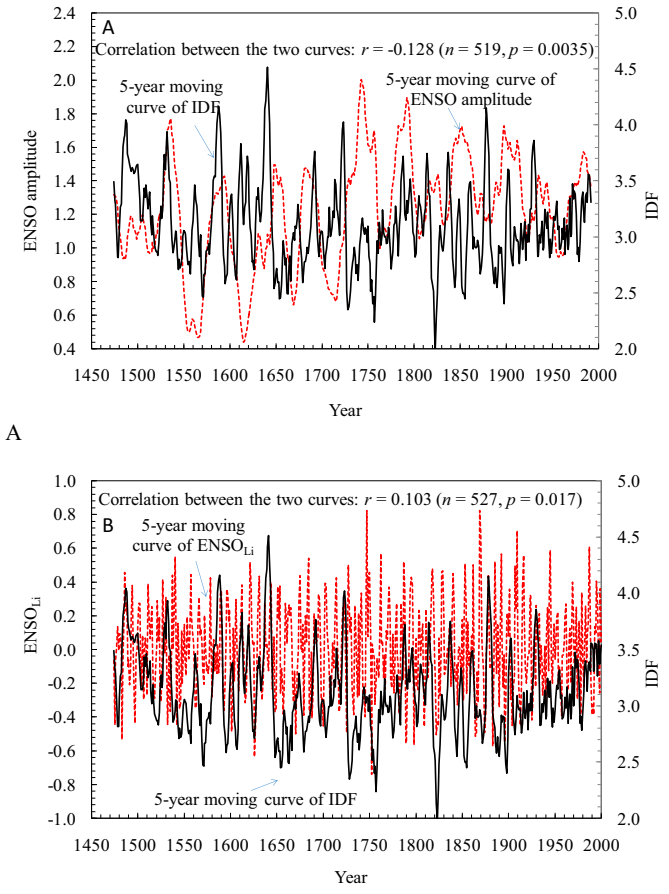
A
Correlation between the two curves: r = -0.128 (n = 519, p = 0.0035)
5-year moving curve of IDF
5-year moving curve of ENSO amplitude
ENSO amplitude
IDF
Year
B
Correlation between the two curves: r = 0.103 (n = 527, p = 0.017)
5-year moving curve of ENSOLi
5-year moving curve of IDF
ENSOLi
IDF
Year

Fig. 5. The comparison of the IDF_{19} variation with those of ENSO amplitude (A) and $ENSO_{Li}$ (B). Only the two 5-year moving curves are shown.

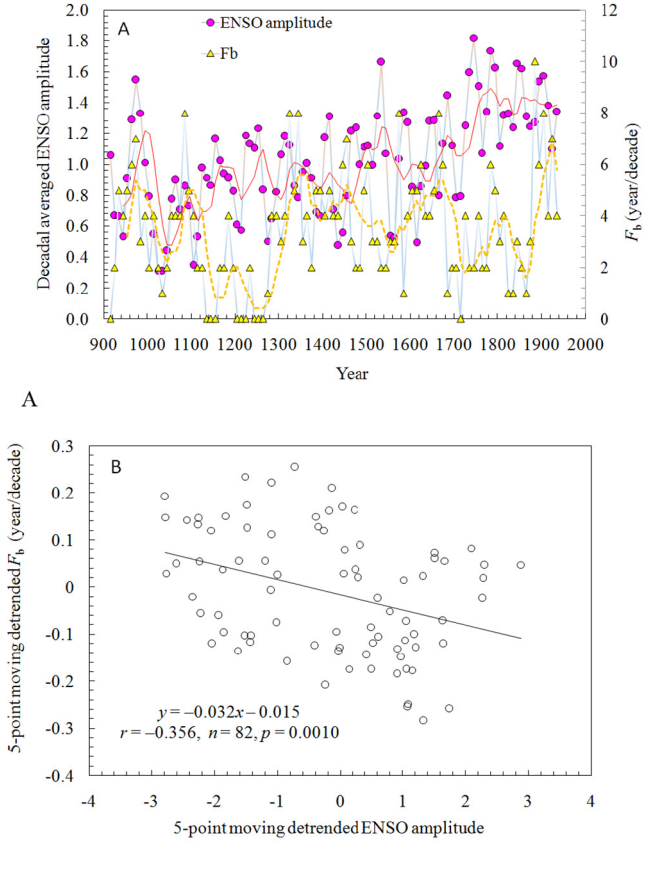

Fig. 6. The variations in F_b and ENSO amplitude (A), and the correlation between F_b and ENSO after a 5-year moving treatment (B).

important factor controlling the variability of summer precipitation in China, especially in the Yellow River basin (e.g., Huang and Wu, 1989; Lan et al., 2002; Hao et al., 2007). As mentioned earlier, the IDF is a proxy expressing summer precipitation variability available from 1470 CE to 2000 (CMA, 1981). We related the averaged value of the IDF at 19 sites in the Yellow River basin (IDF_{19}) to ENSO amplitude and $ENSO_{Li}$ to show how the ENSO influences drought and flooding conditions in the Yellow River basin in the period 1470 CE–1938, the overlap period of the IDF and LBE data. The comparison of the IDF_{19} variation with those of ENSO amplitude and $ENSO_{Li}$ is shown in Fig. 5A and B, respectively, where the 5-year moving curves are fitted. The 5-year moving IDF_{19} is negatively correlated with ENSO amplitude, with $r = -0.128$ ($n = 519$, $p = 0.0035$), significant at $p < 0.01$; the 5-year moving IDF_{19} is positively correlated with $ENSO_{Li}$, with $r = 0.103$ ($n = 527$, $p = 0.017$), significant at $p < 0.05$. According to the definition, IDF = 1 means large flood, and IDF = 6 means large drought; the lower the $ENSO_{Li}$ is, the stronger the La Niña event. According to the definition, the lower value of the $ENSO_{Li}$ means a stronger La Niña event, which may cause higher summer rainfall and flood magnitude, and thus the IDF is lower. Therefore, the positive correlation between IDF and $ENSO_{Li}$ means that during a low $ENSO_{Li}$ year, namely, a stronger La Niña year, the historical summer precipitation would occur, causing a larger magnitude of flood discharge. Hence, the negative correlation between IDF_{19} and ENSO amplitude indicates that when the ENSO amplitude increase (or decrease), the summer precipitation and the resulting flood discharge would decrease (or increase).

For years from 924 CE to 1938, we counted the number of LBE years for each decade, and then calculated the frequency of the LBE (F_b, in year/decade). The variations in F_b and the decadal average of ENSO amplitude are shown in Fig. 6A, where the 5-point moving curves for both variables are fitted. It is seen clearly that, after 1100 CE, the two curves show anti-phase variations, namely, when the ENSO amplitude increases (or decreases), F_b decreases (or increases). After a linear detrending treatment to the data of F_b and the decadal average of the ENSO amplitude, we plotted the 5-point moving F_b against 5-point moving ENSO amplitude in Fig. 6B, which indicates a significant negative correlation, with $r = -0.356$ ($n = 82$, $p = 0.0010$). The results indicate that the ENSO amplitude variation may be one of the causes for the F_b variation.

5. Discussion

5.1. Explanation of the mechanism that the La Niña events influence the occurrence of the LYR LBE

Many studies focused on the influences of ENSO on the summer monsoon and rainfall over China in general (e.g., Fu and Teng, 1988; Huang and Wu, 1989; Ju and Slingo, 2009; Zhang et al., 1996; Tao and Zhang, 1998; Chen et al., 2006; Li, 2008; Li and Ma, 2011), and on rainfall and streamflow in the Yellow River basin in particular (e.g., Lan et al., 2002; Hao et al., 2007; Lin and Lu, 2009; Yuan et al., 2016; Li and Zeng, 2013). Based on the reconstructed annual precipitation since 1736 using the Qing Dynasty imperial palace archives and the reconstructed data of El Niño Index (1525–1987) (Quinn and Neal, 1992), Hao et al. (2007) studied the relation between precipitation over the middle and lower Yellow River basin and El Niño events. They found that there were 92 El Niño years from 1736 to 2002, of which 68 have negative precipitation anomaly in the same year or the following year, accounting for 73.9% of the total El Niño events. Of the 68 years, there

were 42 years in which the negative precipitation anomaly occurred in the same year, and there were 26 years in which the negative precipitation anomaly occurred in the following year. Based on instrumental data from 1920 to 2000, Lan et al. (2002) studied the influence of ENSO events on the annual streamflow of the upper Yellow River. They found that, of the 28 El Niño years, there are 21 dry (anomaly $< -10\%$) and very dry (anomaly $< -20\%$) years, in which an El Niño event occurred either in the same year or in the previous year, indicating that 21 (75%) of the 28 El Niño years caused dry and very dry conditions in annual streamflow. Of the 14 La Niña influenced years, there are 10 wet (anomaly $> 10\%$) and very wet years (anomaly $> 20\%$), in which a La Niña event occurred either in the same year or in the previous year, indicating that 10 (71.4%) of the 14 La Niña influenced years caused wet and very wet conditions in annual streamflow.

The relation between ENSO and summer precipitation and streamflow in the northern China and Yellow River basin has been well established. On the other hand, the relation between the LYR levee breachings and streamflow has also been well established because all the levee breachings were caused by large floods overflowing the top of the levee (for LBE_1) or by large floods approaching the top of the levee (for LBE_2). Through the control on summer rainfall and therefore on floods in the Yellow River, La Niña events influence the occurrence of LBEs and CSEs in the LYR. Many researchers have studied the mechanism of how the ENSO influence precipitation in China. Lin and Lu (2009) found that the relationship between ENSO and the rainfall in eastern China is established through two teleconnections: one is related to the western North Pacific (WNP) anticyclonic anomaly in the lower troposphere leading to enhanced precipitation in the Yangtze River valley, and the other is related to the southward displacement of the Asian jet stream (AJS) in the upper troposphere resulting in suppressed precipitation in the Huaihe River-Yellow River valleys. Many results indicate that the ENSO influences rainfall over China through its influence on the Asian summer monsoon (e.g., Fu and Teng, 1988; Huang and Wu, 1989; Ju and Slingo, 2009; Zhang et al., 1996; Tao and Zhang, 1998; Li, 2008; Li and Ma, 2011). Lan et al. (2002) showed that through the ENSO's effect on the summer west Pacific subtropical high (SWPSH), the teleconnection between ENSO and Yellow River precipitation and streamflow is established. Zhang et al. (2009) found that the sea surface temperature (SST) anomalies of the western Pacific warm pool influence the eastern Asian Summer Monsoon, and thereby controls the variation in the precipitation in the Yellow River basin. The SST anomalies in tropical Indian Ocean influence the Indian Summer Monsoon (Wang and Fan, 1999), which in turn control the precipitation the summer precipitation in the Yellow river basin. The Niño 3.4 index, defined as the SST anomalies in the Niño 3.4 region (170°W–120°W, 5°S–5°N), is an indicator to determine the conditions of El Niño and La Niña events (Trenberth and Stepaniak, 2001). We found that the Niño 3.4 index is closely related with a number of atmospheric circulation indices controlling the precipitation and water discharge in the Yellow River basin. Through a correlation analysis based on the observed data, we established a cause-effect chain between Niño 3.4 index and the occurrence of LBEs as follows: the decreased Niño 3.4 index in association with the increased possibility of La Niña event and the weakened West Pacific Warm Pool → the increased intensity of Asian Summer Monsoon → the increased water vapor flux to the upper and middle Yellow River basin → the increased precipitation → the increased water discharge of the LYR → the increased frequency of levee breaching. Here the variable before "→" is the cause of the variable after "→".To support this inference, we performed correlation analysis between a number of atmospheric circulation variables including Niño 3.4 index (data are available through Climate Prediction Center of National Oceanic and Atmospheric Administration, USA (http://www.cpc.ncep.noaa.gov/)), the temperature anomaly of the West Pacific Pool (WPWPTA, data from Zhang et al. (2009)), the Indian Summer Monsoon index (ISM) defined by Wang and Fan (1999) (data are available through international Pacific Research Center at the University of Hawaii, Honolulu, USA (http://apdrc.soest.hawaiii.edu/projects/monsoon/)); the Eastern Asian Summer monsoon Index (SMI) defined by Guo et al. (2004) (data from Guo et al. (2004)) and the water cycle variables of the Yellow River including the longitudinal summer water vapor flux to the Yellow River basin (LVF) (data from Li et al. (2012)), the annual precipitation over the Yellow River basin above Huayuankou station (P_m) and the natural annual water discharge (Q_{wn}). The observed data of the above variables are from the period 1951–2006. The results show that the Niño 3.4 index is significantly correlated with WPWPTA, with $r = 0.366$ ($p < 0.01$), and the WPWPTA is in turn significantly correlated with SMI, with $r = -0.622$ ($p < 0.01$). Furthermore, the LVF is significantly correlated with SMI, with $r = -0.639$ ($p < 0.01$). In the meantime, SMI is significantly correlated with P_m and Q_{wn}, with $r = 0.315$($p < 0.05$) and $r = 0.381$ ($r < 0.01$), respectively. Similarly, the ISM is significant correlated with Niño 3.4 index, with $r = -0.476$ ($p < 0.01$). The ISM is also significantly correlated with LVF ($r = 0.255$, $p < 0.05$) and with P_m ($r = 0.473$, $n = 0.01$). Hence, the above-mentioned cause-effect chain is well supported.

To further reveal the relation between the ENSO and the channel instability of LYR expressed by F_b, we performed period analysis for the $ENSO_{Li}$ and F_b time series, respectively, using the method of Morlet wavelet analysis, to see if there are some common periods. The results are shown in Fig. 7. Four periodities in the variation in $ENSO_{Li}$ are identified from Fig. 7A, namely, the two major periods of 700 years and 400 years and two minor periods of 40 years and 10 years. Two periods in the variation in F_b are identified from Fig. 7B, namely, a major period of 40 years and a minor period of 10 years. Hence, $ENSO_{Li}$ and F_b share two common periods of 40 and 10 years. Obviously, the 10-year period in F_b reflects the well-known El Niño/Southern Oscillation alternating between anomalously warm (El Niño) and cold (La Niña) conditions in the tropical Pacific at intervals of 2–8 years (D'Arrigo et al., 2005; Deser et al., 2010), which may control the occurrence of LBEs in the LYR. Another period, the 40-year one, also plays a role in controlling the occurrence of LBEs. These results further support the casual relation between $ENSO_{Li}$ and F_b.

5.2. The levee breaching events during the non-La Niña years

Although there are many LBEs that occurred during La Niña years, there are still many LBEs that occurred during the non-La Niña years. Therefore, it is not sufficient to only consider the breaching events during the La Niña years, and a comparison should be made between the La Niña and non-La Niña years. Here, the non-La Niña years are those with $ENSO_{Li} > -0.5$. The results of comparison are shown in Table 3. There are 303 La Niña years and 712 non-La Niña years. Of the 303 La Niña years, there are 131 years without LBEs, accounting for 43.2%; and there are 172 LB years influenced by La Niña, accounting for 56.8%. Of the 712 non-La Niña years, there are 472 years without LBEs, accounting for 66.3%, and there are 240 years with LBEs, accounting for 33.7%. Therefore, the difference between the La Niña influenced years and the non-La Niña influenced years is significant, further indicating that the La Niña is an important factor controlling the occurrence of LBEs in the LYR.

5.3. Influence of human activity

As shown in Fig. 4, the $ENSO_{Li}$ can only explains 50% of the variance in F_b, indicating that there are other factors responsible for the F_b variation. One of these factors is human activity. Two major types of human activity should be considered. The first is related with levee construction and maintenance. The good maintenance of artificial levees would reduce the risk of LBE occurrence; if the levees had not been maintained and strengthened for many years due to war, social unrest and financial difficulties, the LBE frequency would increase. In history,

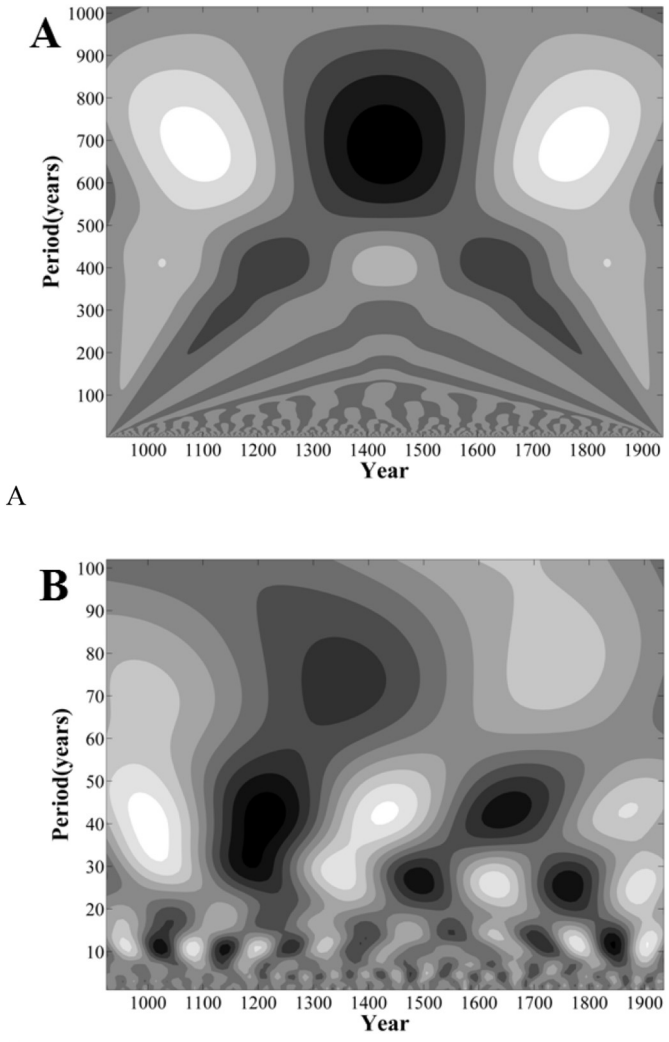

Fig. 7. Wavelet power spectrum of the hydrologic variables including (A) $ENSO_{Li}$ (924 CE (letft side)–1938 (right side)) and (B) F_b (920 CE–1930s), the time of each decade is represented by the mid-year, namely, 925 CE (left (side)–1935 (right side)).

Table 3
The occurrence of levee breachings during La Niña and the non-La Niña years.

Item	With and without LBEs	Number of years	Frequency (%)
La Niña years	Without LBEs	131	43.2
($ENSO_{Li} < -0.5$)	With LBEs	172	56.8
	Sub-total	303	100.0
Non-La Niña years	Without LBEs	472	66.3
($ENSO_{LI} > -0.5$)	With LBEs	240	33.7
	Sub-total	712	100.0

the government of various dynasties paid high attention to the Yellow River because the utilization of water resources and protection of flood disasters directly concerned national socio-economic development and society stability. After 924 CE, there were 3 times of large scale channel training in the LYR in history, namely, the project by Daxia Liu in 1493 CE and the project by Jixun Pan from 1565 to 1592 during the Ming Dynasty and the project by Fu Jin from 1677 to 1692 during the Qing Dynasty (WGYRCC, 1982). Although these projects effectively stabilized the river channel, the beneficial effect could not last long because the huge amount of SSL from the Loess Plateau did not change. Not long after the projects, the channel became instable again. The second is related with the man-induced land-use changes in the drainage basin, which is reflected by the boundary between the agricultural and animal husbandry areas in the Loess Plateau. As annual precipitation decreases from south to north in the Loess Plateau region, the southern part is dominated by agriculture and the northern part by animal husbandry. The boundary between the two parts is an important limit in land-use. Actually, this boundary is the northern limit of the main agricultural area (LLMAA). Influenced by human activity and climate change, the northward and southward shifts of this limit occurred in history. To quantify this shift, we use the line from the lower Weihe River and the Yellow River from the Weihe River–Yellow River confluence to Mengjin (see Fig. 1) as a "baseline", and calculate the average distance between this base line and the line of the northern limit of the major agricultural area in different periods in history (Zhu, 1991; Xu, 2001). This average distance is then used an indicator to express the shift of the LLMAA. The cultivation of hillslopes will push northward the northern boundary of agricultural area and thereby greatly intensifies soil erosion and sediment yield, increasing the suspended sediment load (SSL) to the LYR and accelerating the bed rise due to sedimentation. As a result, the LBE risk will increase. On the other hand, the southward intrusion of nomadic people that usually lived in the steppe zones lying to the north of the Loess Plateau will expand the pastoral area southward, reducing the SSL to the Yellow River and therefore the LBE risk. In addition, there is another type of LBEs. In history, the man-induced levee breaching, namely, digging up the artificial levee and letting the flood inundate the enemy's troops, was sometime used as attacking or defensive means during a war. According to the historical records, these man-induced levee breaching events occurred 7 times in the LYR, in 281 BCE, 225 BCE, 896 CE, 918 CE, 923 CE, 1128 CE and 1938 CE (Wen, 2001). Only the last two occurred during the period studied. They are also the CSEs listed in Table 2, included in the CSEs from the Yellow River Water Conservancy Commission (1959) study. The two years were not La Niña-influenced years. The population in the Loess Plateau is an index that comprehensively reflects the human impact on environment and therefore on the LYR SSL, channel sedimentation and LBEs. Hence, two indices of human activity, the NLMAA and the historical population in the Loess Plateau region, were used in the present study. We also considered the timing of the three large scale channel training.

The time-resolution of the LBE and ENSO data and human activity data are quite different. The time-resolution of the former is rather high, but that of the available data of the latter are very low because there are only 10 data points for the NLMAA and 11 data points for the population. Therefore, it is impossible to match each levee breaching event to these human activity variables. For the time-being, what we are able to do is making a comparison between the temporal variations in the F_b and LERI with the variations in human activity variables to see if there are some meaningful links. The study took two steps: the first is to determine how the variation in F_b is influenced by human activity and the second is to determine how the variation LBEs is influenced by human activity in the background of ENSO changes. As mentioned earlier, the LERI (LBE-ENSO responding index) is an indicator that reflects how the LBEs responded to the ENSO, we studied how the variation of LERI may be related to the variations in the variables of human activity.

Fig. 8A shows the temporal variations in F_b, NLMAA, the population and the timing of the three large scale channel training. It is seen that the population was positively correlated with time (the year) ($r = 0.813$, $n = 13$, $p = 0.00072$), the NLMAA was positive correlated with time ($r = 0.740$, $n = 11$, $p = 0.013$); and in the meantime, the F_b was also positively correlated with time ($r = 0.189$, $n = 104$, $p = 0.054$). These overall trends indicate that the human activity strengthening with time may exert some influence on the F_b. However, the synchronicity of the variations is rather weak, implying the influence of human activity expressed by the above three variables is not the

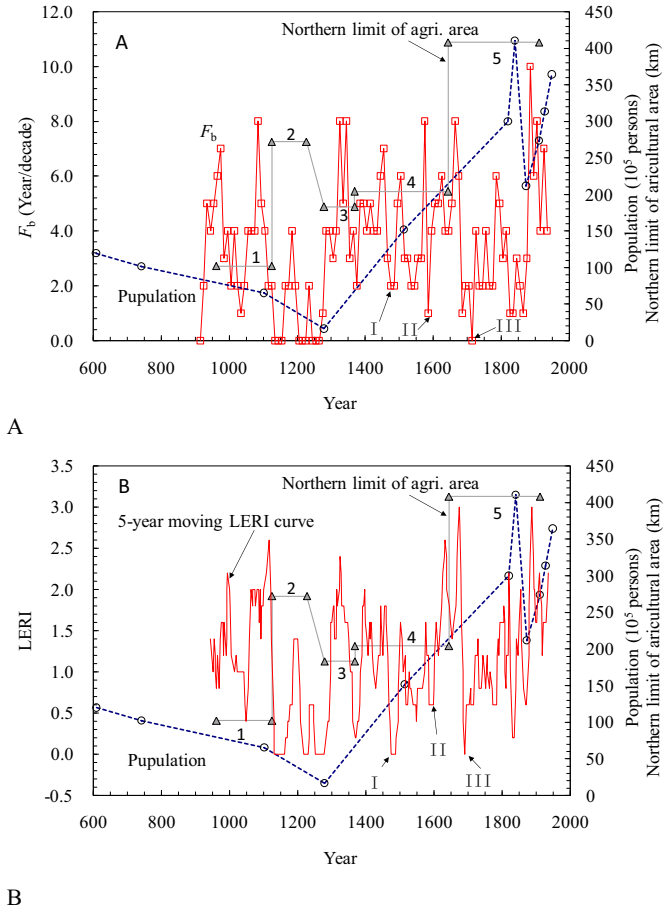

Fig. 8. (A). Comparison of variation in the the frequency of LBE years (F_b) with those in population, northern limit of agricultural area and the timing of three LYR training and control projects. (B). Comparison of variation in LERI (only the 5-point moving curve is shown) with those in population, northern limit of agricultural area and the timing of three LYR training and control projects. In panels A and B, the Roman numbers of I, II and III are referred to as the three LYR training and control projects led by Daxia Liu, Jixun Pang and Fu Jin, respectively. The Arabic numbers are referred to the northern limit of agricultural area in different periods: 1. Tang Dynasty (962–1125); 2. Northern Song, Liao and West Xia Dynasties (1125–1227); 3 Yuan Dynasty (1279–1368); 4. Ming Dynasty (1368–1644); 5. Qing Dynasty (1644–1911). The northern limit of the main agricultural area (NLMAA) is referred to as the averaged distance of the NLMAA to the west-east line of the Weihe River and part of the Yellow River (see Fig. 1).
(Data from Xu, 2001). The data of Loess Plateau population are from Chen (1990).

determinant factor of the LBEs. It is notable that the low value of population around 1200 CE was coincidental with the low value of F_b and that the three LYR training and control projects led by Daxia Liu (I), Jixun Pang (II) and Fu Jin (III) were well coincidental with the low values of F_b, also indicating that the human activity had some influence on the occurrence of LBEs.

To reveal how the LERI responded to the changing human activity, we made a comparison of the temporal variation in LERI with those in population, northern limit of the main agricultural area (NLMAA) and the timing of three LYR training and control projects (Fig. 8B). After three major LYR training and control projects, the LERI sharply declined from a peak value to a low value. After the two project led by Daxia Liu and Fu Jin, the LERI declined to 0. This fact indicated that through channel training, artificial levee system was strengthened, the main channel became more stable and the LYR's flood releasing capacity greatly increased, thereby reducing the LERI significantly. It can be seen that from Period 1 (Tang Dynasty) to Period 2 (Northern Song, Liao and Xixia dynasties), the NLMAA shifted northward, the LERI increased; from Period 2 to Period 3 (Yuan Dynasty), the NLMAA shifted southward, the LERI decreased; from Period 3 to Period 4 (Ming Dynasty), the NLMAA shifted northward slowly, the LERI increased slightly; from Period 4 to Period 5 (Qing Dynasty), the NLMAA shifted southward greatly, the LERI in the late Period 5 increased sharply. Notably, during and after the LYR training and control project led by Fu Jin (marked as III in Fig. 8), the LERI remained at low values for many years, but afterward, the artificial levee system were not well maintained and repaired because of financial difficulty of the central government. This factor, together with the northward shift of the NLMAA, led to a high LERI in the late Period 5. The Loess Plateau population in Yuan Dynasty (1279–1368) is the lowest since 609 CE in the Sui Dynasty. Responding to this, the LERI also reached a minimum. During the period from 609 CE to the Yuan Dynasty, the population was negatively correlated with time (the year) ($r = -0.97$, $n = 6$, $p = 0.015$), and so was the LERI ($r = -0.42$, $n = 100$, $p = 0.000016$). After this lowest point, the population was positively correlated with time (the year) ($r = 0.87$, $n = 8$, $p = 0.0050$), and so was the LERI (after 5-moving treatment) ($r = 0.12$, $n = 201$, $p = 0.080$).This fact indicates that the increase (or decrease) in population would cause increase (or decrease) in the LERI.

5.4. Further study

In the present study, the information in the historical records of LBEs has not been fully used. As mentioned earlier, we did not consider how many times and sites of LBEs occurred in each La Niña influenced year in the present study. As shown in WGYRCC (1982), for some years the times of LBEs within a year and the sites of LBE along the river were recorded. In further study, this information should be taken into consideration because in a strong La Niña year, the magnitude of flood would be larger and more times or sites of LBE may be expected to occur.

In the present study, we explained the mechanism of how the LBEs are influenced by the La Niña through a statistical analysis on the teleconnections between a number of indices related with atmospheric circulations and the precipitation and water discharge in the Yellow River basin. This is not sufficient. In the future, some physically based simulation model should be aimed to better reveal the mechanism.

According to the methodology used, although the published databases of ENSO based on tree-rings reconstruction in North America (Li et al., 2012) has annual resolution, this does not necessarily mean that the real ENSO value was known for a given year because a smoothing treatment on data was used by Li et al. (2012). When the ENSO time series is matched with the LBEs year by year, some uncertainty would be added to the result. However, the value may still reflect the relative magnitude of a given year more or less, especially for the strong La Niña or El Niño years. When the ENSO data are correlated with F_b index, which is at 10-year scale, the effect of the above problem would become much smaller. More study is needed in the future to better solve this problem.

We found in the present study that the in the year after a La Niña-influenced year, a LBE may occur. The mechanism for this needs to be studied in the future. One of the possible explanations is that in a La Niña-influenced year, the amount of winter snowfall would be high, which causes a large snowmelt flood in the next year that would increase the risk of LBE occurrence. To test this, we studied the LYR floods during spring. The snowmelt induced spring floods occur in the upper Yellow River, and after the adjustment due to channel storage along a river length of nearly 3000 km, the discharge at Huayuankou station on the LRY is rather low and cannot be regarded as a flood. The discharge during the spring months is low, and almost no peak can be seen. Therefore, the effect of spring flood of the LYR on bank breaching is negligibly small. In the future, the mechanism that La Niña causes an

increase in floods in the next summer should be studied.

6. Conclusions

The El Niño/Southern Oscillation (ENSO) not only influences the summer precipitation and streamflow of the Yellow River basin, but also influenced the historical channel instability expressed by the frequency of artificial levee breaching events (LBEs). From 924 to 1938, there are 303 La Niña influenced years (ENSO variability < -0.5), of which 172 (56.8%) are related to the occurrence of LBE. This indicates that the LYR channel instability was influenced by La Niña. We found that 13 (61.9%) of the 21 CSEs were influenced by the La Niña events. The decadal LBE frequency (F_b) and decadal average of ENSO amplitude show anti-phase variations since 1100 CE. The correlation between them is significant at $p < 0.001$, after a linear detrending treatment. Through the control on summer rainfall and therefore on floods in the Yellow River, La Niña events influence the occurrence of the LBEs and CSEs in the LYR.

Acknowledgments

The financial support from the National Natural Science Foundation of China (grant no. 41330751 and 41371037) is gratefully acknowledged. We are grateful to Dr. Jinbao Li and coworkers for their reconstructed ENSO data, which make the present study possible; to the anonymous reviewers, whose comments and suggestions are valuable for revising the manuscript.

Appendix A. Supplementary data

Supplementary data to this article can be found online at https://doi.org/10.1016/j.catena.2019.01.012.

References

Braganza, K., Gergis, J.L., Power, S.B., Risbey, J.S., Fowler, A.M., 2009. A multiproxy index of the El Nino-Southern Oscillation, A.D. 1525–1982. J. Geophys. Res. Atmos. 114, D05106. https://doi.org/10.1029/2008JD010896.

Chang, W.Y.B., King, G., 1999. Centennial climate changes and their global associations in the Yangtze River (Chang Jiang) Delta, China and subtropical Asia. Clim. Res. 2, 95–103.

Chen, B. (Ed.), 1990. On the Population of the Loess Plateau of China. Science Press, Beijing (122 pp., in Chinese).

Chen, W., Kang, L.H., Wang, D., 2006. The coupling relationship between summer rainfall in China and Global Sea surface temperature. Climatic Environ. Res. 11 (3), 259–269 (in Chinese).

Chen, Y., Overeem, I., Kettner, A.J., Gao, S., Syvitski, J.P.M., 2015. Modeling flood dynamics along the superelevated channel belt of the Yellow River over the last 3000 years. J. Geophys. Res. Earth Surf. 120, 1321–1351. https://doi.org/10.1002/2015JF003556.

Chien, N., Zhou, W.H., 1965. The Lower Yellow River Channel Processes. Science Press, Beijing (in Chinese).

Chiew, F.H.S., McMahon, T.A., 2002. Global ENSO-streamflow teleconnection, streamflow forecasting and interannual variability. Hydrol. Sci. J. 47, 505–522.

Chiew, F.H., Piechota, T.C., Dracup, J.A., McMahon, T.A., 1998. El Nino/Southern Oscillation and Australian rainfall, streamflow and drought: links and potential for forecasting. J. Hydrol. 204 (1), 138–149.

CMA (China Meteorological Administration), 1981. Yearly Charts of Dryness/wetness in China for the Last 500-year Period. Chinese Cartographic Publishing House, Beijing (in Chinese).

Cook, E.R., Woodhouse, C., Eakin, C.M., Meko, D.M., Stahle, D.W., 2004. Long-term aridity changes in the western United States. Science 306, 1015–1018.

Cook, E.R., et al., 2008. North American Summer PDSI Reconstructions, Version 2a. IGBP PAGES/World Data Center for Paleoclimatology Data Contribution Series # 2008-046 NOAA, NGDC Paleoclimatology Program, 2008.

Cook, E.R., et al., 2009. Tree Ring 500 Year ENSO Index Reconstructions. IGBP PAGES/World Data Center for Paleoclimatology Data Contribution Series # 2009-105 NOAA/NCDC Paleoclimatology Program, Boulder CO, USA.

D'Arrigo, R., Cook, E.R., Wilson, R.J., Allan, R., Mann, M.E., 2005. On the variability of ENSO over the past six centuries. Geophys. Res. Lett. 32, L03711.

Deser, C., Alexander, M.A., Xie, S.P., Phillips, A.S., 2010. Sea surface temperature variability: patterns and mechanisms. Annu. Rev. Mar. Sci. 2, 115–143.

Dilley, M., Heyman, B.N., 1999. ENSO and disaster: droughts, floods and El Nino/Southern Oscillation warm events. Disasters 19 (3), 181–193.

Dong, J., Liu, L.M., 2000. The relationship of temperature and precipitation in China and the ocean temperature in the Equatorial East Pacific. Meteorology 26 (2), 25–28 (in Chinese).

Editorial Commission for Physical Geography in China, 1982. Physical Geography in China: Historical Geography. Science Press, Beijing (in Chinese).

Fu, C.B., Teng, X.L., 1988. Climate anomalies in China associated with E1 Ni?o/Southern Oscillation. Chin. J. Atmos. Sci. 12 (s1), 133–141. https://doi.org/10.3878/j.issn.1006-9895.1988.t1.11. (in Chinese).

Fu, G., Yu, J., Yu, X., Ouyang, R., Zhang, Y., Wang, P., Min, L., 2013. Temporal variation of extreme rainfall events in China, 1961–2009. J. Hydrol. 487, 48–59.

Grinsted, A., Moore, J.C., Jevrejeva, S., 2004. Application of the cross wavelet transform and wavelet coherence to geophysical time series. Nonlinear Process. Geophys. 11 (5–6), 561–566.

Guo, Q., Cai, J.N., Shao, X.M., Sha, W.Y., 2004. Studies on the variations of East Asian summer monsoon during AD 1873–2000. Chin. J. Atmos. Sci. 28 (2), 206–215 (in Chinese).

Hao, Z.X., Zheng, J.Y., Ge, Q.S., 2007. Precipitation cycles in the middle and lower Yellow River. Acta Geograph. Sin. 62 (5), 537–544 (in Chinese).

Huang, R.H., Wu, Y.F., 1989. The influence of ENSO on the summer climate change in China and its mechanism. Adv. Atmos. Sci. 6, 21–31.

Jiang, W.G., Li, J., Wang, L., 2006. Compositive analysis of global flood disaster from 1950 to 2004. J. Beijing Normal Univ. (Nat. Sci.) 42 (5), 530–533 (in Chinese).

Jones, P.D., 1988. The influence of ENSO on global temperatures. Climate Monitor 17 (3), 80–89.

Ju, J., Slingo, J.M., 2009. The Asian Summer Monsoon and ENSO. Quart. J. Roy. Meteor. Soc. 121, 447–462.

Jotheri, J., Allen, M.B., Wilkinson, T.J., 2016. Holocene avulsions of the Euphrates River in the Najaf area of Western Mesopotamia: impacts on human settlement patterns. Geoarchaeology 31, 175–193.

Kiladis, G.N., Diaz, H., 1989. Global climatic anomalies associated with extremes in the Southern Oscillation. J. Clim. 2, 1069–1090.

Lan, Y.C., Ma, Q.J., Kang, E.S., Zhang, J.S., Zhang, Z.H., 2002. Relationship between ENSO cycle and abundant or low runoff in the Upper Yellow River. J. Desert Res. 22 (3), 262–266 (in Chinese).

Li, C., 2008. Coupling mode analysis of summer precipitation in mid-low valley of Yangtze River and sea surface temperature in Northwest Pacific. J. Trop. Oceanogr. 27, 38–44 (in Chinese).

Li, C., Ma, H., 2011. Coupled modes of precipitation over China and the Pacific Sea surface temperature in boreal summertime. Adv. Atmos. Sci. 28, 1201–1214.

Li, C., Zeng, G., 2013. Impacts of ENSO on autumn rainfall over Yellow River loop valley in observation: possible mechanism and stability. J. Geophys. Res. Atmos. 118, 3110–3119. https://doi.org/10.1002/jgrd.50264.

Li, Y.H., Li, D.L., Zhao, Q.Y., 2000. A study on spring rainfall anomaly in Northwest China and Pacific SSTA features in autumn and their correlations. Plateau Meteorol. 19 (1), 100–110 (in Chinese).

Li, J., Xie, S.P., Cook, E.R., Huang, G., D'Arrigo, R., Liu, F., Ma, J., Zheng, X.T., 2011. Interdecadal modulation of El Niño amplitude during the past millennium. Nat. Clim. Chang. 1 (2), 114–118. https://doi.org/10.1038/nclimate1086.

Li, J., Li, D.L., Zhang, J., 2012. Characteristics of water vapor transportation and budget of winter and summer in the Yellow River basin. Plateau Meteorol. 31 (2), 342–350 (in Chinese).

Li, L.P., Song, Z., Wu, N., 2015. Effects of three types of El Nino events on atmospheric circulation over East Asia and following summer precipitation in eastern China. Trans. Chin. Atmos. Soc. 38 (6), 753–765 (in Chinese).

Lin, Z.D., Lu, R.Y., 2009. The ENSO's effect on eastern China rainfall in the following early summer. Adv. Atmos. Sci. 26 (2), 333–342. https://doi.org/10.1007/s00376-009-0333-4.

Liu, J.Y., Zhang, Q., Singh, V.P., Gu, X.H., Shi, P.J., 2017. Nonstationarity and clustering of flood characteristics and relations with the climate indices in the Poyang Lake basin, China. Hydrol. Sci. J. 62 (11), 1809–1824.

Long, Z.X., Li, C.Y., 1999. GCM modeling of the impacts of the ENSO on Estern Asian Summer Monsoon activities. Acta. Meteor. Sin. 57 (6), 663–671 (in Chinese).

McPhaden, M.J., Zebiak, S.E., Glantz, M.H., 2006. ENSO as an integrating concept in Earth science. Science 314, 1740–1745.

Quinn, W.H., Neal, V.T., 1992. The historical record of El Niño events. In: Bradley, R.S., Jones, P.D. (Eds.), Climate since A.D. pp. 623–648 (Routledge).

Tang, Y., Deng, Z., Zhou, X., Cheng, Y., Chen, D., 2008. Interdecadal variation of ENSO predictability in multiple models. J. Clim. 21, 4811–4833.

Tao, S., Zhang, Q., 1998. Response of the East Asian summer monsoon to ENSO events. Sci. Atmos. Sin. 22, 399–407 (in Chinese).

Torrence, C., Webster, P., 1999. Interdecadal changes in the ESNO Monsoon System. J. Clim. 12, 2679–2690.

Trenberth, K.E., 1997. The definition of El Niño. Bull. Am. Meteorol. Soc. 78, 2771–2777.

Trenberth, K.E., Stepaniak, D.P., 2001. Indices of El Niño evolution. J. Clim. 14, 1697–1701.

Wang, B., Fan, Z., 1999. Choice of South Asian summer monsoon indices. Bull. Amer. Meteor. Soc. 80, 629–638.

Wang, Y., Su, Y., 2013. Influence of solar activity on breaching, overflowing and course-shifting events of the Lower Yellow River in the late Holocene. The Holocene 23 (5), 656–666.

Ward, P.J., Eisner, S., Flörke, M., Dettinger, M.D., Kummu, M., 2014. Annual flood sensitivities to El Niño–Southern Oscillation at the global scale. Hydrol. Earth Syst. Sci. 18 (1), 47–66.

Wen, X., 2001. Manmade bank breachings of the Yellow River. United Daily News (May 18, Page 3, Jinan, in Chinese).

WGYRCC (Writing Group of "A Brief History of Yellow River Water Conservancy", Yellow River Water Conservancy Commission), 1982. A Brief History of Yellow River Water

Conservancy. Water Conservancy and Electric Power Press, Beijing (in Chinese).
Woodward, J.C., Williams, M.A.J., Garzanti, E., Macklin, M.G., Marriner, N., 2015. From source to sink: exploring the Quaternary history of the Nile. Quat. Sci. Rev. 130, 3–8. https://doi.org/10.1016/j.quascirev.2015.10.022.
Xu, J.X., 2001. Historical bank-breachings of the lower Yellow River as influenced by drainage basin factors. Catena 45 (1), 1–17.
Xu, J.X., 2012. Temporal variation in summer monsoon intensity since 1873 and its influence on runoff in the drainage area between Hekouzhen and Longmen, Yellow River basin, China. Clim. Chang. 112 (2), 283–298.
Yellow River Water Conservancy Commission, 1959. The People's Yellow River. Publishing House for Yellow River Water Conservancy, Zhengzhou (in Chinese).
Yi, L., Yu, H., Ge, J., Lai, Z., Xu, X., Qin, L., Peng, S., 2012. Reconstructions of annual summer precipitation and temperature in north-central China since 1470 AD based on drought/flood index and tree-ring records. Clim. Chang. 110 (1–2), 469–498. https://doi.org/10.1007/s10584-011-0052-6.
Yuan, F., Yasuda, H., Berndtsson, R., Bertacchi Uvo, C., Zhang, L., Hao, Z., Wang, X., 2016. Regional sea-surface temperatures explain spatial and temporal variation of summer precipitation in the source region of the Yellow River. Hydrol. Sci. J. 61 (8). https://doi.org/10.1080/02626667.2015.1035658.
Zhang, D., 1988. The method for reconstruction of the dryness/floodness series in China for the last 500 years and its reliability. In: Zhang, J. (Ed.), The Reconstruction of Climate of China for Historical Times. Science Press, Beijing, pp. 18–31.
Zhang, R., Sumi, A., Kimoto, M., 1996. Impact of El Niño on the East Asian monsoon: a diagnostic study of the 86/87 and 91/92 events. J. Meteorol. Soc. Jpn. 74, 49–62.
Zhang, Z., Gong, D., He, X., Guo, D., Feng, S., 2009. Reconstruction of the western Pacific warm pool SST since 1644 AD and its relation to precipitation over East China. Sci. China Ser. D Earth Sci. 52 (9), 1436–1446.
Zhao, W.L. (Ed.), 1996. The Sediment of the Yellow River. Publishing House for Yellow River Water Conservancy, Zhengzhou (in Chinese).
Zhu, S.G., 1991. The change in vegetation distribution. In: Yang, Q.Y., Yuan, B.Y. (Eds.), The Changes in Natural Environment in the Loess Plateau Region. Science Press, Beijing, pp. 143–152 (in Chinese).
Zhu, Q.G., Teng, Y., Xu, G.Q., 2000. The possible mechanism of the effects of SSTA in north Pacific on East China summer rainfall. J. Nanjing Inst. Meteorol. 23 (1), 1–8.
Zou, L., Ni, Y.Q., 1997. Impact of ENSO on the variability of the summer monsoon over Asia and the summer rainfall in China. J. Trop. Meteorol. 3 (4), 306–314 (in Chinese).